Electroencephalography in patients with disturbed level of consciousness

Bogdan Florea

Supervisors:

Professor Sándor Beniczky

Professor László Vécsei

University of Szeged, 2021

Doctoral School of Clinical Medicine

List of scientific papers that cover the topic of the dissertation:

I. **Bogdan Florea**, Simona Alexandra Beniczky, Helga Demény, Sándor Beniczky. Semiology of Subtle Motor Phenomena in Critically Ill Patients. Seizure. 2017 May;48:33-35. doi: 10.1016/j.seizure.2017.03.018. Epub 2017 Mar 30.

II. **Bogdan Florea**, Remus Orasan, Cristian Budurea, Ioan Patiu, Helga Demeny, Cosmina Ioana Bondor, László Vécsei, Sándor Beniczky. EEG spectral changes induced by hemodialysis. Clinical Neurophysiology Practice 6 (2021). doi: 10.1016/j.cnp.2021.03.006.

III. Daniel Kroeger, **Bogdan Florea**, Florin Amzica. Human Brain Activity Patterns Beyond the Isoelectric Line of Extreme Deep Coma. PLoS One. 2013 Sep 18;8(9):e75257. doi: 10.1371/journal.pone.0075257. eCollection 2013.

Introduction

Electroencephalography (EEG) is the most often used functional investigation method in neurology. Its main application is in the field of epilepsy and disturbance of consciousness, because of the cortical origin of the signals. In this PhD project, we focused on the following conditions related to disturbed level of consciousness: epilepsy/status epilepticus, uremic encephalopathy and coma.

Study 1

Subtle phenomena resembling discrete ictal manifestations have been described in patients with nonconvulsive status epilepticus (NCSE) [1]. These subtle motor phenomena consist of discrete phenomena like twitches of the eyelids, face, jaw, extremities or the trunk, head and/or eye deviation, as well as peculiar automatisms [1,2]. Treiman speculated that these subtle motor phenomena occur when the patient experiences such a degree of encephalopathy that an electromechanical dissociation occurs, so that in spite of continuous ictal activity in the brain, only subtle motor phenomena are generated [3].

This term has gained wide acceptance in clinical practice. In the classification of status epilepticus (SE) published by the International League Against Epilepsy (ILAE), this is referred to as "subtle" SE [4,5]. However, its diagnosis is challenging, since these phenomena are subtle and they can also occur in other pathological conditions in critically ill patients [2]. Drugs, particularly anaesthetics and analgesics, can induce myoclonic twitches [6]. It has been suggested that certain features of the subtle movements, like their duration or persistence can help in distinguishing between NCSE and other causes of these phenomena [6]. However, the semiology of these subtle motor phenomena has not been systematically studied yet.

By using EEG as the gold standard, in the first part of our study, we aimed to investigate and describe the semiological features of subtle motor phenomena that occur in critically ill patients, with and without NCSE.

Study 2

There have been controversial reports on EEG changes induced during hemodialysis in patients with chronic kidney disease (CKD). Early observational studies based on visual assessment of the recordings, reported increase in the slow EEG frequency components following hemodialysis: increase in theta activity and appearance of high amplitude delta potentials [7,8].

However, later studies using quantitative spectral analysis methods were not able to confirm these observations [9-12].

EEG changes induced during hemodialysis are important because they may elucidate the pathogenic mechanisms and highlight the risk factors of a neurological complication occurring during or immediately after hemodialysis, coined dialysis disequilibrium syndrome [12-15]. Paradoxically, patients may show deterioration in their general condition toward the end of or immediately following hemodialysis, by developing symptoms such as headache, nausea and vomiting, disorientation, asterixis and involuntary jerking movements. In rare, severe cases, psychosis, generalized tonic-clonic seizures and coma may be seen.

In the second part of our study, our goal was to evaluate quantitative EEG changes induced during hemodialysis, using spectral analysis methods, and to identify risk factors associated with these changes.

Study 3

Regardless of the underlying causes, coma is a state during which the brain reaches a low level of neuronal activity and metabolism. Possible etiologies range from safe and fully reversible pharmacological interventions (such as general anesthesia) to severe, irreversible brain damage. There is virtually no systematic investigation of the cerebral cellular mechanisms at work during coma and attempts to compare pathological and pharmacological etiologies are scarce. It is therefore no surprise that the outcome from coma is often predicted on a statistical basis. Recent results from the laboratory where the study was conducted have highlighted two unexpected findings. First, it was shown that coma induced by a variety of anesthetics presents a time-frame during which the cortex is in a hyperexcitable state that is responsible for the genesis of the burst-suppression (BS) pattern [16]. Second, evidence was reported for the fact that isoflurane-induced BS opens the blood-brain barrier [17]. BS was first described by Swank and Watson [18]. Its main feature at the EEG level consists of quasi-periodical bursts of bilateral high-amplitude slow waves (mainly ,15 Hz) separated by low-amplitude or absent activity lasting from a few seconds to minutes [19]. The first cellular correlates of BS were revealed by Steriade and colleagues [20], demonstrating that EEG bursts were associated with excitatory activities in cortical neurons, while suppression phases were paralleled by absence of cortical network interactions. The same study showed that thalamic neurons displayed spontaneous discharges throughout BS with no apparent correlation to the two phases of BS. Overall, BS was mainly investigated as a

prognostic tool during coma [21]. The common clinical correlate of coma is loss of consciousness and low or absent responsiveness [19]. Although the initial stages (I–II) of coma are comparable to deep sleep [22], deep coma (stages III-IV) corresponds to more profound alterations of brain states, observable at the electroencephalographic (EEG) level [23,24]. Deepening of the coma beyond the BS stage leads to a flat EEG called isoelectric line, which is presumed to be associated with silenced activity in cortical neurons. Such an EEG pattern is considered to be one of the limit points in establishing brain death and in particular clinical conditions it is accepted as the only criterion [25]. The activity of subcortical neurons (e.g. thalamic, hippocampal) has not been studied during EEG isoelectric line, but it might be hypothesized both from the situation encountered during the suppression phase of the BS pattern [20] and from recordings in isolated preparations (such as in vitro), that a rudiment of oscillatory activity might persist in subcortical neurons. Whether this activity can become synchronized and re-emerge at the cortical level is so far unknown.

In the third part of our study, we aimed to demonstrate that a novel brain phenomenon is observable in both humans and animals during coma that is deeper than the one reflected by the isoelectric EEG, and that this state is characterized by brain activity generated within the hippocampal formation. We hypothesized that if cerebral neurons survive through the deepening of coma, then network activity can revive during deeper coma than the one accompanying the EEG isoelectric line by the change in the balance of hippocampal-neocortical interactions.

Methods and materials

Study 1

For the first part of our study, we prospectively recorded and described the type, location and occurrence-pattern/duration of subtle motor phenomena occurring in patients admitted to the Intensive Care Units (ICUs) of three medical centers in Cluj-Napoca, Romania (the Clinical Hospital for Infectious Diseases, the Institute for Heart Disease and the Regional Institute for Gastroenterology and Hepatology).

Inclusion criteria were: critically ill patients, admitted to the ICU, in whom the personnel observed discrete motor phenomena. The study was approved by the Institutional Ethics Committee, and the relatives of the patients gave their informed consent.

To confirm NCSE, EEG was recorded simultaneously with the subtle movements. Video footage and EEG was prospectively recorded for a sufficient duration to capture and characterize the subtle motor phenomena observed by the personnel in the ICU. The minimal duration of the recordings was 30 minutes. When needed, repeated recordings were done. Semiological features were extracted from the video recordings by three board-certified neurologists, with experience in evaluating patients in the epilepsy monitoring units and intensive care units. The following features were logged into the database: (1) type / name of the semiological phenomenon; (2) somatotopical feature, i.e. the part of the body involved; (3) occurrence, i.e. time-related feature. These features were extracted in joint reading sessions, in randomized order from the video-database, blinded to the clinical and electrographic data. EEG was evaluated by two board-certified clinical neurophysiologists, in joint reading sessions, blinded to the clinical data, and we scored the recordings using the Salzburg criteria for NCSE. EEG recordings were considered to confirm NCSE if they satisfied the Salzburg criteria, which have a high sensitivity and specificity [26-28]. Demographic data, diagnosis and final outcome were also entered into the database, besides semiology and EEG.

We used Chi-square test to analyze the difference in occurrence of the semiological features between the patients with NCSE and those without. In case of small cell frequencies (≤ 5) the Fisher's exact test was used.

Study 2

In the second part of our study, we included consecutive patients with CKD, undergoing hemodialysis treatment three times per week at the Nefromed Dialysis Center in Cluj-Napoca. Patients gave their informed consent, and the study has been approved by the Ethics Committee of the Nefromed Dialysis Center.

Hemodialysis treatments were performed on 5008 Fresenius machines with synthetic (helixone) high flux membranes with surfaces adapted to body weight and blood-flow to achieve Kt/V at least 1.4.in 240 minutes. Kt/V is a way of measuring dialysis adequacy: K stands for the dialyzer clearance, the rate at which blood passes through dialyzer, expressed in milliliters per minute (mL/min), t stands for time, V represents the volume of water a patient's body contains. One third of the patients had online-hemodiafiltration targeting at least 21 l substitution per treatment. Bicarbonate solutions with glucose were used: Na=138 mmol/l, K=2 mmol/l, Ca=1,5mg/dl, bicarbonate=30-34 mEq/l, glucose=1 g/l. Each hemodialysis session had a duration of 210 –270 minutes. At the end of the hemodialysis sessions, patients generally experienced mild symptoms, such as malaise and fatigue, but these were not severe and specific enough to be considered as DDS.

EEGs were recorded for the entire duration of the hemodialysis sessions, with an EBNeuro Galileo EEG equipment, using scalp electrodes Ag/AgCl EasyCap (B10-S-200) placed according to the international 10-20 system[29]. Normal awake activities such as speaking, eating or watching television were allowed. The sampling frequency was 256 per second. At the beginning and at the end of each hemodialysis sessions, an experimenter verbally alerted the patients and, after a short conversation with them, to keep vigilance, the patients were required to stay relaxed with open eyes for 2-3 minutes. Patients and EEGs were real-time monitored by the experimenter, to assess the vigilance. Of these periods, where the patient was awake, with open eyes, artifact-free epochs of 12 seconds [30] were identified and subsequently analyzed.

EEG was evaluated by two board-certified clinical neurophysiologists, in joint reading sessions, blinded to all clinical data. Signals were digitally filtered 0.5–30 Hz. To minimize any muscle artefacts, the central electrodes have been chosen for quantitative analysis: C3 (central left) and C4 (central right). An average of the values was calculated Cm = (C3+C4)/2, for all the further studies. We used common average reference. We analyzed the following frequency bands: Delta (0.5–4 Hz), Theta (4–8 Hz), Alpha (8–13 Hz) and Beta (13–30 Hz). We calculated the Total

Power (all bands), the Relative Power for each band (ratio of the power in the frequency band and the Total Power), and the Power Ratio between the slow and the high frequency powers: (Delta+Theta)/(Alpha+Beta).

We measured the End-Tidal Carbon Dioxide ($EtCO_2$, CO_2 concentration of the expired air) through a Stardust nasal cannula and assessed the pulse, EKG, respiratory rate (RR), and pulse oximetry with a LifeSense Nonin Capnograph. At the start of the hemodialysis sessions, the body mass was recorded, blood tests for bicarbonate (ECO_2), serum Na, K, Ca, serum creatinine, glucose and urea were performed and blood pressure (BP) was measured. The pH was recorded on the left anatomical snuffbox with a portable dermatology pH-meter Hanna Instruments (model HI 99181). The comorbidities of the patients were also recorded.

For statistical analysis, we calculated the median (± standard deviation [SD]) for those parameters with normal distribution and with median 25^{th}–75^{th} percentile) for parameters that did not have normal distribution. We used Kolmogorov-Smirnov test for assessment of the normality of distribution. For each patient, two values for the Alpha, Theta, Delta and Beta parameters were obtained from the spectral analysis, one at the beginning and one at the end of hemodialysis. The initial and final values were compared by calculating the difference of each data pair and comparing it to zero, using Student test for paired samples when data had normal distribution and Wilcoxon test when distribution was not normal. In univariate analysis Pearson or Spearman coefficient of correlation were used to analyze the relationship between two quantitative variables. The univariate analysis was followed by multivariate analysis. We used linear regression model for multivariate analysis. Each EEG measurement parameter was the dependent variable, in a separate linear regression model. As independent variables, we used the variables that proved to be significantly correlated with the EEG measurement parameters in the univariate analysis. Probability $p<0.05$ was considered significant. The analysis was performed using SPSS and Microsoft Excel.

Study 3

In the third part of our study, we used EEG recordings from one human patient on one hand, and double simultaneous intracellular recordings in the cortex and hippocampus, combined with EEG, in cats, on the other hand.

All experimental procedures were performed according to NIH guiding principles and were also approved by the committee for animal care of the Laval University (Comité pour la protection des animaux de l'Université Laval, CPAUL). For the human recordings, written consent was obtained from the family in order to use the recordings performed during the patient's treatment for publication; no experimental paradigm was implemented on the patient. The Committee for Ethics of the Unirea (Regina Maria) Medical Centre approved of the use of the recordings for publishing purposes.

Experiments were performed on 26 cats (2.5–4.5 kg) of both sexes. The surgical procedures were described in detail elsewhere [16]. After the initial dose of ketamine-xylazine (15 mg/kg and 3 mg/kg, respectively), animals were paralyzed (gallamine triethiodide), and anesthesia was switched to isoflurane (1.3–1.5%). After a stable baseline recording containing continuous slow and ample EEG waves, the isoflurane was increased to 4% in order to induce νC patterns. During the experiments vital parameters were continuously monitored and maintained within physiological limits: body temperature (37±0.2˚C), expired CO_2 (3.7±0.2%), respiration rate (20–30 strokes/min) and heart rate (<110 beats/min). Through craniotomy, we exposed the suprasylvian gyrus, where intracellular pipettes and field electrodes were lowered into the cortex and in the hippocampus using stereotaxic coordinates. The hippocampal pipettes were lowered through the suprasylvian gyrus and lateral ventricles aiming at the CA3 region of the hippocampus (AP+5; L+5.5; H+7.5 - in parallel to the midline). Neuroanatomical evidence for the placement of the recording electrodes was obtained for a few cells by staining neurons with intracellular injection of Lucifer yellow (3%, Invitrogen; dissolved in a 1 M $LiCl_2$ solution, Sigma). The intracellular filling was achieved by applying hyperpolarizing pulses (500 ms at 1 Hz) of 1–3 nA for 10–15 min. At the end of the experiments, the brains were perfused with 4% paraformaldehyde and stored in paraformaldehyde and 30% sucrose for 2–3 days. Sections of 75 μm were taken and cells were revealed using a Zeiss confocal laser-scanning microscope (LSM 5 PASCAL, Zeiss, Oberkochen, Germany).

Human EEG recordings were performed in monopolar configuration, with the reference placed on the earlobes and crosslinked. Due to the supine position of the critically ill patient, occipital electrodes could not be placed in the 10–20 classical configuration. Instead, they were positioned more laterally, closer to the temporal ones. Filtering was set for all channels between 0.1 and 300 Hz, with the notch filter on. The analysis was performed with software from WaveMetrics Inc.

(Igor software, Oregon, USA), and relies on time relationships between the recorded voltage time series. Most of the results are presented as event- or spike-triggered averages. They were obtained after extracting from the intracellular or extracellular field/EEG potentials sweeps synchronized with the triggering event (action potentials or extreme of a particular waveform) and averaging them. This provided the statistical evidence for interactions between the discharge in the reference channel and the field/EEG potential variations of the target channel. Crosscorrelograms were derived in order to detect time relationships between events of similar origin recorded from different channels. The procedure consisted in detecting events in two simultaneously recorded channels. The events in one channel were kept as time reference (time zero), and the time lags of the events in the other channel with respect to each event in the reference channel were plotted in a histogram.

Results

Study 1

In the first part of our study, 60 consecutive patients (24 female), aged between 6 days and 80 years (mean: 40.7, median: 46.5 years) were analysed. The patients had a Glasgow Coma Scale between 3 and 9 (mean: 4.9; median: 5).

Fourteen out of the 60 patients (23%) with subtle motor phenomena in the ICU had NCSE confirmed by EEG. Table 1 shows diagnoses and the final outcomes in the subgroups of patients with and without NCSE. There was no significant difference between the two subgroups concerning demographic data, diagnosis and outcome. Antiepileptic drug therapy was instituted significantly more often ($p = 0.02$) in the subgroup of patients with subtle convulsions and NCSE confirmed by EEG (Table 1).

Table 1. Diagnoses and outcome in the sub-groups of critically ill patients with subtle motor phenomena, with and without NCSE.

	NCSE (N=14)	**Coma without NCSE (N=46)**
Diagnoses		
Autoimmune	1	1
Post-anoxic	4	18
Creutzfeldt Jakobs Disease	1	4
Arterio-venous malformation	0	2
Metabolic	2	3
Neuroinfection	3	7
Traumatic brain injury	0	3
Tumor	1	1
Vascular	2	6
Not determined	0	1
Outcomes		
Institution of AED medication	12	24
Survived without decreased function	7	13
Survived with decreased function	2	10
Deceased	5	23

N, number of patients; NCSE, nonconvulsive status epilepticus; AED, antiepileptic drug

Table 2 shows the semiological features in the sub-groups of patients with and without NCSE. In both sub-groups, the most common phenomenon was discrete myoclonic muscle-twitching, which often occurred almost continuously or in clusters. The second most common phenomenon in both sub-groups was discrete tonic muscle activation, with a duration between 1–30 seconds. Besides these, subtle automatisms and eye-deviation were identified in both sub-groups. None of the semiological features could distinguish between the sub-groups of critically ill patients with NCSE and those without.

Table 2. Semiological features in the sub-groups of patients with- and without NCSE.

Subtle seizure phenomena	n(%)	Body part	Occurrence
		NCSE (N=14)	
Myoclonus	10 (71)	Tongue: 2 Perioral: 2 Face: 2 Upper limbs: 6 Lower limbs: 4	Almost continous: 3 Sporadic: 2 In clusters: 5 (20, 4–30)*
Tonic muscle activation	3 (21)	Upper limbs: 1 Lower limbs: 3	Duration: 5 s (1–10 s)**
Automatisms	2 (14)	Oro-facial: 1 Upper limbs: 1	Almost continous: 1 Sporadic: 1
Eye deviation	2 (14)		Almost continous: 1 Sporadic: 1
		Coma without NCSE (N=46)	
Myoclonus	19 (41)	Eyelid: 3 Face: 1 Upper limbs: 16 Lower limbs: 12 Axial: 1	Almost continous: 5 Sporadic: 8 In clusters: 6 (9, 4–120)*
Tonic muscle activation	19 (41)	Face: 1 Upper limbs: 16 Lower limbs: 12 Axial: 1	Duration: 4 s (1–30 s)**
Automatisms		Oro-facial: 4 Upper limbs: 3 Lower limbs: 2	Almost continous: 2 Sporadic: 6
Eye deviation	4 (9)		Almost continous: 2 Sporadic: 6

* median, range; ** mean, range

NCSE, nonconvulsive status epilepticus; N, number of patients; n(%), number of patients exhibiting a certain phenomena

Study 2

In the second part of our study, we included and analyzed 56 consecutive patients (20 female), aged between 32 and 86 years (mean: 59.82±12.76, median: 60.5 years). The patients had been receiving hemodialysis between 1 month and 192 months (mean: 61.41±51.60, median: 42 months), and had the following comorbidities: high blood pressure (50 patients; 50.0%), diabetes (18 patients; 32.1%), hepatopathies (10 patients; 17.9%), thyroid disease (8 patients; 14.3%), epilepsy (3 patients; 5.4%), history of traumatic brain injury (3 patients; 5.4%). Table 3 shows the baseline biochemical and clinical parameters of the patients.

Table 3. Baseline biochemical and clinical parameters at the start of the hemodialysis session (N=56).

Parameter, unit	Value	Reference range
Body weight, kg (mean±SD)	79.66±17.2	
Serum bicarbonate, mmol/L (mean [range])	20 (18, 22)	22–29 mmol/L
Glycemia, mg/dL (mean [range])	97 (84, 129)	60–99 mg/dL
Serum calcium, mg/dL (mean [range])	8.97 (8.6, 9.49)	8.6–10 mg/dL
Serum creatinine, mg/dL (mean [range])	8.43 (6.63, 10.29)	<1.2 mg/dL
Serum potassium, mmol/L (mean [range])	5.35 (4.7, 5.9)	3.3–5.1 mmol/L
Serum natrium, mmol/L (mean [range])	137 (135, 140)	136–145 mmol/L
Urea, mg/dL (mean [range])	122 (100, 139)	<43 mg/dL
Blood urea nitrogen, mg/dL (mean [range])	57 (47, 65)	<20 mg/dL
Systolic blood pressure, mm Hg (mean [range])	140 (123.5, 157.5)	
Dyastolic blood pressure, mm Hg (mean [range])	77 (68, 80)	
Pulse, bpm (mean±SD)	71.82±9.33	
Skin pH (mean [range])	6.03 (5.81, 6.39)	
pCO_2 exhaled, % (mean [range])	35 (31.5, 39)	

SD, standard deviation

Hemodialysis resulted in a significant increase in Total EEG Power (Table 4). Spectral analysis showed increase in Relative Power of Delta band and an increase in the Power Ratio of the slow EEG components toward the end of hemodialysis (Table 4).

Table 4. EEG changes during hemodialysis, demonstrated by spectral analysis

Parameter	Start of hemodialysis	End of hemodialysis	p
Total Power, μV² (mean [range])	14.54 (7.17, 20.7)	19.41 (12.98, 39.29)	**<0.001***
RP Delta, % (mean±SD)	0.32±0.14	0.37±0.19	**0.035**$^{+}$
RP Theta, % (mean [range])	0.14 (0.09, 0.2)	0.12 (0.09, 0.21)	0.967*
RP Alpha, % (mean [range])	0.24 (0.14, 0.34)	0.2 (0.13, 0.32)	0.146^{+}
RP Beta, % (mean [range])	0.24 (0.19, 0.38)	0.23 (0.12, 0.32)	0.071^{+}
Power Ratio (mean [range])	0.94 (0.57, 1.6)	1.08 (0.68, 2.04)	**0.033***

* Wilcoxon rank-sum test; + Student t test for paired samples

RP, Relative power; Power Ratio, (Delta+Theta)/(Alpha+Beta)

Significant differences are marked in **bold**.

Multivariate analysis showed that EEG changes induced by hemodialysis were associated with younger age, recent start of hemodialysis, uremia and lower level of glycaemia (Table 5).

Table 5. Correlation between the biochemical and clinical parameters of the patients and the spectral EEG changes: significant correlation in univariate and multivariate analysis.

Dependent variable*	Independent variable	Univariate analysis		Multivariate linear analysis	
		Correlation coefficient	p	b (95% CI)	p
Total Power	Age	-0.39	**0.003**	-1.456 (-2.734; -0.179)	**0.026**
	Bicarbonate	-0.28	**0.041**	-	
	Urea	0.37	**0.005**	-	
RP Delta	Total duration of dialysis (months)	0.34	**0.011**	-	-
	Glycemia	-0.34	**0.013**	-0.001 (-0.002; 0)	**0.036**
	BW	-0.31	**0.020**	-	-
RP Theta	Age	-0.27	**0.044**	-0.002 (-0.003; 0)	**0.030**
	Total duration of dialysis (months)	-0.32	**0.015**	-0.001 (-0.001; 0)	**0.011**
RP Alpha	Glycemia**	0.38	**0.004**	-	
	Body weight	0.29	**0.030**	-	
RP Beta	Glycemia	0.27	**0.047**	0.001 (0; 0.001)	0.047
Power Ratio	Age	-0.28	**0.039**	-	-
	Glycemia**	-0.34	**0.012**	-	-
	Urea	0.41	**0.002**	0.033 (0.008; 0.058)	**0.011**

* EEG parameter difference end-start of dialysis; ** nonlinear relationship

RP, relative power; EEG, electroencephalography; CI, confidence interval

Significant differences are marked in **bold**.

Study 3

EEG phenomena in deep coma

One of the main challenges in clinical practice is the fact that the interpretation of the EEG of a comatose patient is often hindered by the lack of information concerning the dynamic progression of the patient's state. Such an exceptional case was represented by the EEG pattern displayed below.

The patient was admitted to the emergency service after cardiorespiratory arrest and successful resuscitation. By the time of his arrival at the hospital he was unconscious and presented

quasiperiodic generalized convulsions. He was administered antiepileptic medication (carbamazepine 3 times 200 mg per day, diazepam 3 times 10 mg per day, and thiopental i.v. 175 mg/kg/h) and this reduced the convulsions to quasiperiodic jerks. EEG recordings performed at this time showed a pattern like the one depicted in Figure 1.

Figure 1. Typical pattern of EEG recorded from temporal (T3 and T4) and modified occipital (O1'and O2') derivations.

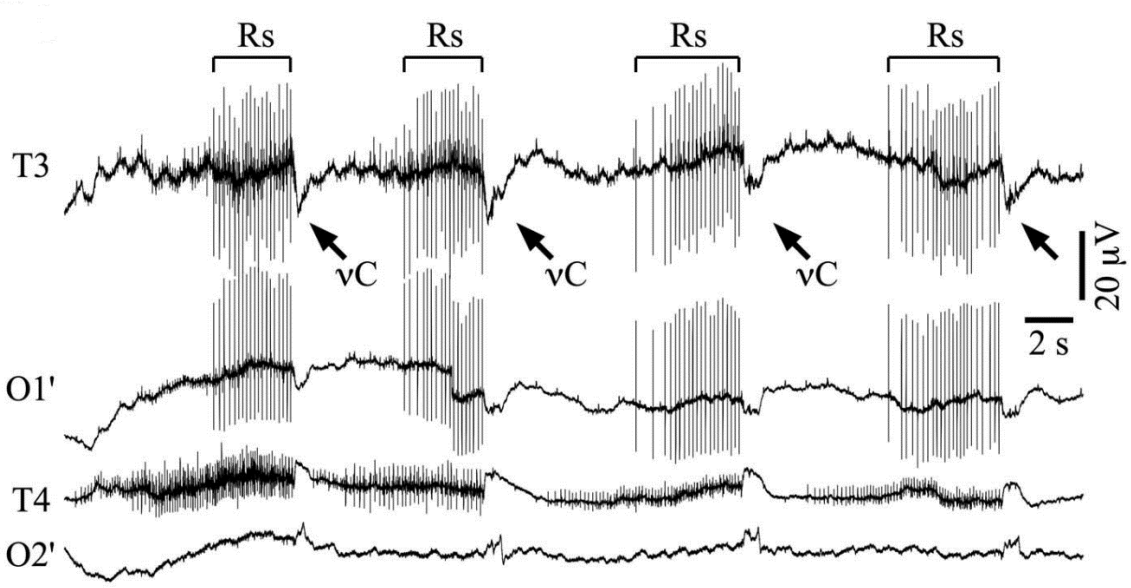

The pattern is dominated by ripples (Rs; bracket lines) and n-complexes (νCs; oblique arrows). The recording also contains cardiac contamination, as often in comatose patients.

Most unusually, it was dominated by bursts of rhythmic spike-like discharges (average frequency of 5.8±0.9 Hz; values are given as mean ± standard deviation), somewhat akin in shape and frequency to hippocampal ripple events (Rs), with each burst lasting for several seconds. They seemed to originate independently in several foci. We give below the example of those recorded in the T4 derivation (Figure 2, left panel) and those of O1' (Figure 2, right panel). Each trace represents the average of 5000 ripple events.

Figure 2. Averaged ripples (n = 5000) on the EEG recording of a patient in deep coma

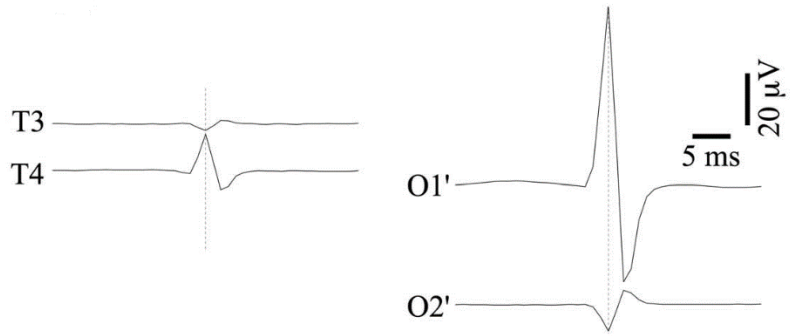

Left panel: Positive peak detection of Rs in the T4 derivation and averaging of all signals reveals no potentials in the occipital leads (not shown) and a reverted, less ample, ripple in T3. Right panel: similarly, positive peak detection in the O1' derivation and averaging of all signals shows only a small and reverted ripple in O2'.

Ripples originating at one location were also recorded by contralateral electrodes with reversed polarity. The simultaneity of the two waveforms and their opposed polarity has been encountered in situations with an interposed dipole, although a definite conclusion is difficult to draw at this point. Moreover, there was no time relationship between ripples generated at different recording sites (Figure 3), indicating that these events were not propagating through cerebral circuits but rather being generated by independent oscillatory structures and recorded by our electrodes through volume transmission.

Figure 3. Cross-correlogram between ripples in T4 and O1' shows no time relationship

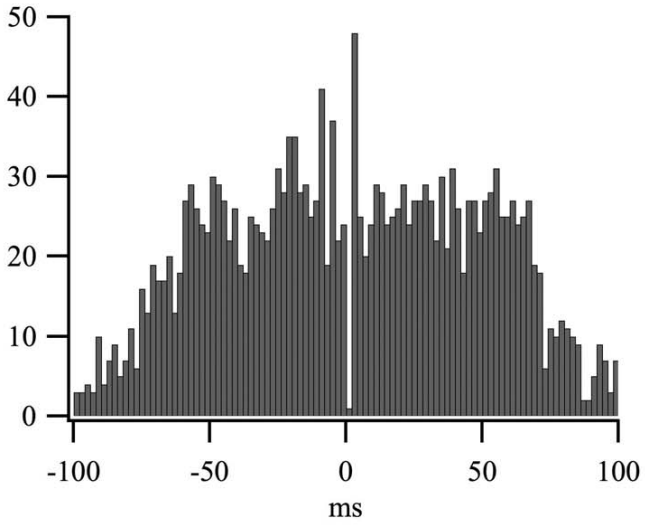

Other peculiar waveforms present during these recordings were ample and slower deflections that occurred simultaneously with the motor jerks of the patient (indicated by oblique arrows in Figure 1). For reasons that will become obvious further, we call this waveform niu-complex (νC). Its aspect is further detailed in Figure 4, where averaged νCs (n=350) are characterized by consistent polarity in any of the recorded leads (positive on the right, negative on the left). νCs appeared pseudo-rhythmically every ~10 s (average time interval of 9.3±2.7 s; n =350).

Figure 4. Averaged νCs (n = 350) on the EEG recording of a patient in deep coma

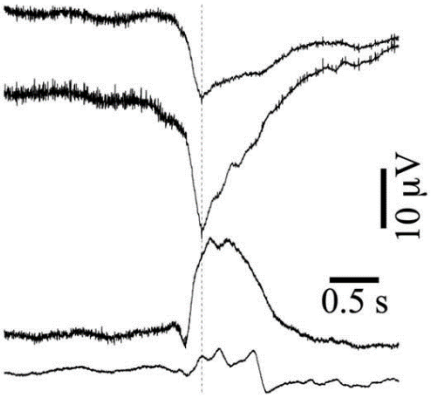

The negative peak of νCs in the O1' derivation was detected and sweeps of 4 s around that time marker were extracted from each derivation and averaged.

After 6 days spent in this state, the antiepileptic medication was discontinued and, after passing through a period of isoelectric activity, the EEG assumed a pattern of burst-suppression (Figure 5) with frequent stereotyped burst shapes as described elsewhere [16]. This latter pattern is usually present during deep coma [19], and in this case was achieved by removing pharmacological agents such as thiopental reputed to deepen coma.

Figure 5. Same patient, after removing antiepileptic drugs (carbamazepine, diazepam and thiopental) displays a pattern of burst-suppression

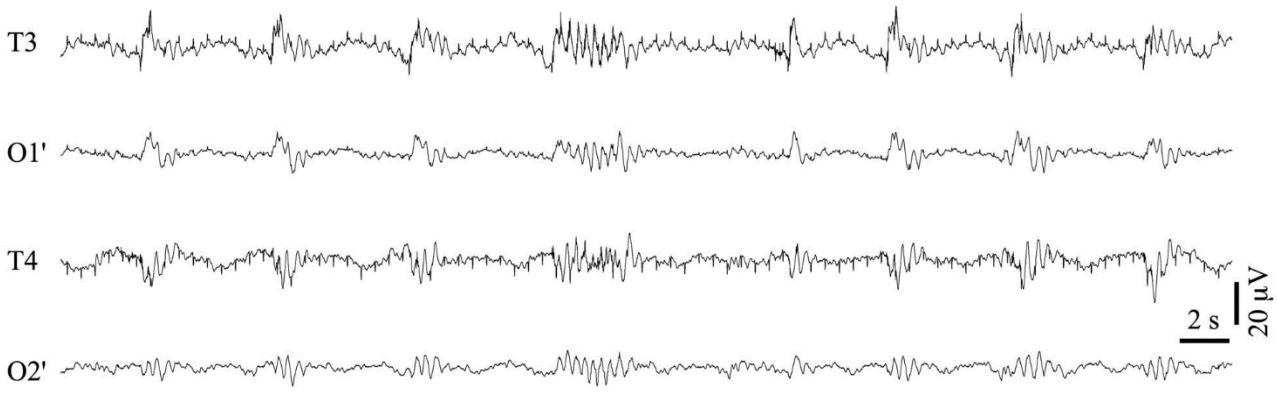

Contamination of the EEG by the electrocardiogram is visible especially in the temporal leads. In this figure, all potentials are depicted with positivity upwards.

Therefore, we hypothesized that under antiepileptic medication the patient was in a deeper state of coma. Moreover, this state was accompanied by novel EEG patterns that are not described in the literature. We therefore planned a series of experiments with laboratory animals in order to elucidate the cellular mechanisms underlying this behavior.

EEG phenomena in comatose animals

Figure 6 (A–D) summarizes the essential EEG features accompanying the deepening of coma, as obtained with progressive doses of the anesthetic isoflurane applied in cats.

Figure 6. EEG patterns during wakefulness and diverse degrees of loss of consciousness: cat EEG recording during application of various concentrations of isoflurane

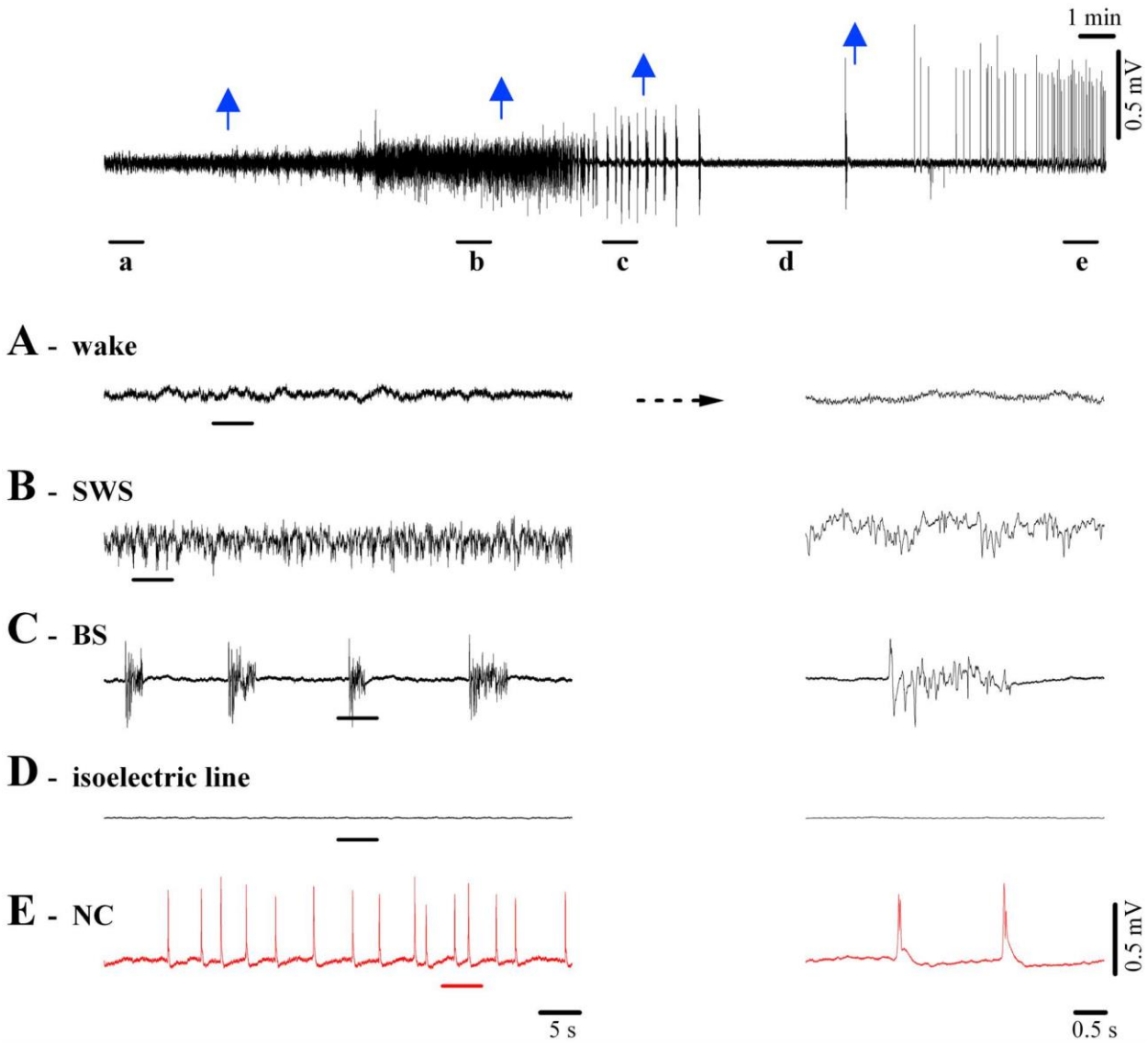

The top panel depicts the complete sequence with arrows indicating the applications of increasing anesthesia; the underlined epochs are expanded below. (A) Undrugged preparation displaying low amplitude, fast (mostly >15 Hz) EEG. (B) Slow-wave sleep-like (SWS) pattern after 1% isoflurane, characterized by higher amplitude slow waves dominated by delta oscillations (<4 Hz). (C) Burst-suppression (BS) induced with 2% isoflurane showing alternating sequences of isoelectric line and bursting episodes. The latter are very similar to SWS patterns (see detail at right). (D) A further increase in the isoflurane concentration (3%) establishes a stable isoelectric line portraying the absence of phasic events. Only very low-amplitude activities can be observed at high gain. (E) Isoflurane at 4% elicits a revival of quasi-rhythmic spiky potentials of high amplitude, which we propose to call n-complexes (or Niu-complexes; νC). In this figure, all potentials are depicted with positivity upwards.

Wakefulness (Figure 6A) and sleep-like oscillations (Figure 6B) have been extensively studied and their cellular and ionic substrates are well understood [31]. Briefly, the EEG of wakefulness displays a relatively low amplitude and contains fast waves with a frequency spectrum generally above 15 Hz. Slow-wave sleep (SWS)-like patterns were induced with an initial dose of isoflurane of 1% (first blue arrow in Figure 6). The EEG pattern of SWS is dominated by slow oscillations (<1 Hz) [32] intermingled with other rhythms such as delta (<4 Hz) and spindles (7–15 Hz) [31].

The BS pattern shown in Figure 6C, first described by Swank and Watson [18], is associated with deep coma and generally develops during anesthesia (in our case, isoflurane at 2% applied at the 2nd arrow in Figure 6), hypoxia, cardiac arrest, drug-related intoxications, childhood encephalopathies, hypothermia, etc. [33-38]. The neurophysiological mechanisms responsible for generating BS patterns remained elusive for many years. Recently we have shown that BS induced with various anesthetics (isoflurane, propofol, barbiturates) is associated with a state of cortical hyperexcitability in that the bursts of the BS pattern can be triggered by subliminal stimuli reaching the hyperexcitable cortex [16].

Figure 6D depicts the EEG isoelectric line following increased doses of isoflurane anesthesia (3% at the 3rd arrow in Figure 6), reflecting a further deepening of the coma. Such EEG patterns are considered to portray “electrocerebral silence” and are one of the hallmarks in establishing brain death. Therefore, in clinical conditions, the presence of a prolonged isoelectric line in a comatose patient is, among others, one of the determinants of a fatal diagnosis [25].

The novelty reported in this study is that through an application of anesthetics beyond what is required for the induction of the isoelectric line (isoflurane >3.5%) we obtained a re-vitalization of activity in the brain, reflected by the EEG (Figure 6E). This activity was characterized by sharp EEG waves occurring quasi-rhythmically at frequencies below 1 Hz. Since this EEG wave has been unknown until now, we propose to call it n-complex (Nu-complex, νC), in deference to EEG tradition and its resemblance to the Greek letter “n”. Given that such activity patterns have not been reported before, essential questions as to the site of genesis and underlying cellular mechanisms need answering.

Hippocampal activities – recordings of ν-Complexes in cats

At the EEG level, νCs were characterized by amplitudes of 1.3 mV (60.2, n = 70) and duration of 129 ms (±25). Since νCs were clearly expressed in the EEG, we assumed that they would

primarily reflect cortical activities. Furthermore, our field potential (FP) recordings performed in all cortical areas (primary as well as associative ones) also displayed high amplitude νCs (3.4±0.4 mV) (Figure 7A, upper trace). These FP events consisted almost exclusively of negative potentials in deep cortical layers (Figure 7B5, upper trace), reflecting massive and synchronous cellular excitation. It became apparent from these recordings that νC-activity shared features with exclusively hippocampal phenomena such as the sharp waves during resting wakefulness and slow-wave sleep [39], and slow intrinsic spikes under urethane anesthesia [40]. Additional similarities were observed between νCs and less hippocampal-specific patterns such as epileptic interictal spikes [41]. Whether or not νCs were also present in the hippocampus or other subcortical structures was investigated with double field potential recordings. Virtually all tested structures (thalamus, basal forebrain, brainstem and hippocampus) displayed activities time related with EEG νCs (not shown). However, among all subcortical structures, hippocampal νCs exhibited by far the greatest amplitude. Moreover, νCs from all other structures displayed a time-lag trailing hippocampal νC events by at least 10 ms, suggesting that the hippocampus might be the key structure for generating νCs. In more detail, measuring the time lags between the peaks of νCs recorded as field potentials we obtained the following values: basal forebrain was delayed with respect to the hippocampus by 14.2±3.7 ms (n= 240 νCs, data pooled from 3 animals), brainstem was delayed by 18.4±5.1 ms (n =240, 3 animals), and thalamus (lateral pulvinar nucleus) was delayed by 9.8±4.6 ms (n = 240, from 3 animals).

Simultaneous cortical and hippocampal field potential recordings also emphasized another activity exclusively present in this subcortical structure: faster ripple oscillations that were observable even during the cortical isoelectric line (Figure 7). Indeed, these ripple oscillations were a constant feature starting with the state of BS (Figure 7B1) and continuing throughout the transition to the EEG isoelectric line (Figure 7B2–4) and νC state (Figure 7B5). In all recordings of progressions from BS to νC state (n = 14) hippocampal ripple frequency slowed down continuously starting in the low beta range (15.8±0.9 Hz) during BS and ending within the delta range (2.2±0.7 Hz). In parallel with the slowing of the oscillatory frequency we noted an increase in the amplitude of the ripples by an average factor of 10, suggesting a progressive increase in the synchronization within hippocampal networks during ripple activity. Interestingly, νCs appeared to reset the amplitude scale for ripples (Figure 7B5) in that the first event after a νC was dramatically smaller, whilst subsequent ripples displayed successively larger amplitudes.

Although ripple activity was not overtly visible in cortical recordings, we noticed that at higher amplifications and with the benefit of simultaneous hippocampal field potentials, one could distinguish coherent phasic potentials even in the cortical field potential (Figure 7B3–5). This observation raised the question as to whether such FP events portray true intracellular oscillations by cortical neurons or are merely the reflection of hippocampal dipoles.

Figure 7. Isoflurane induction of deep coma, including the EEG isoelectric line and νC state

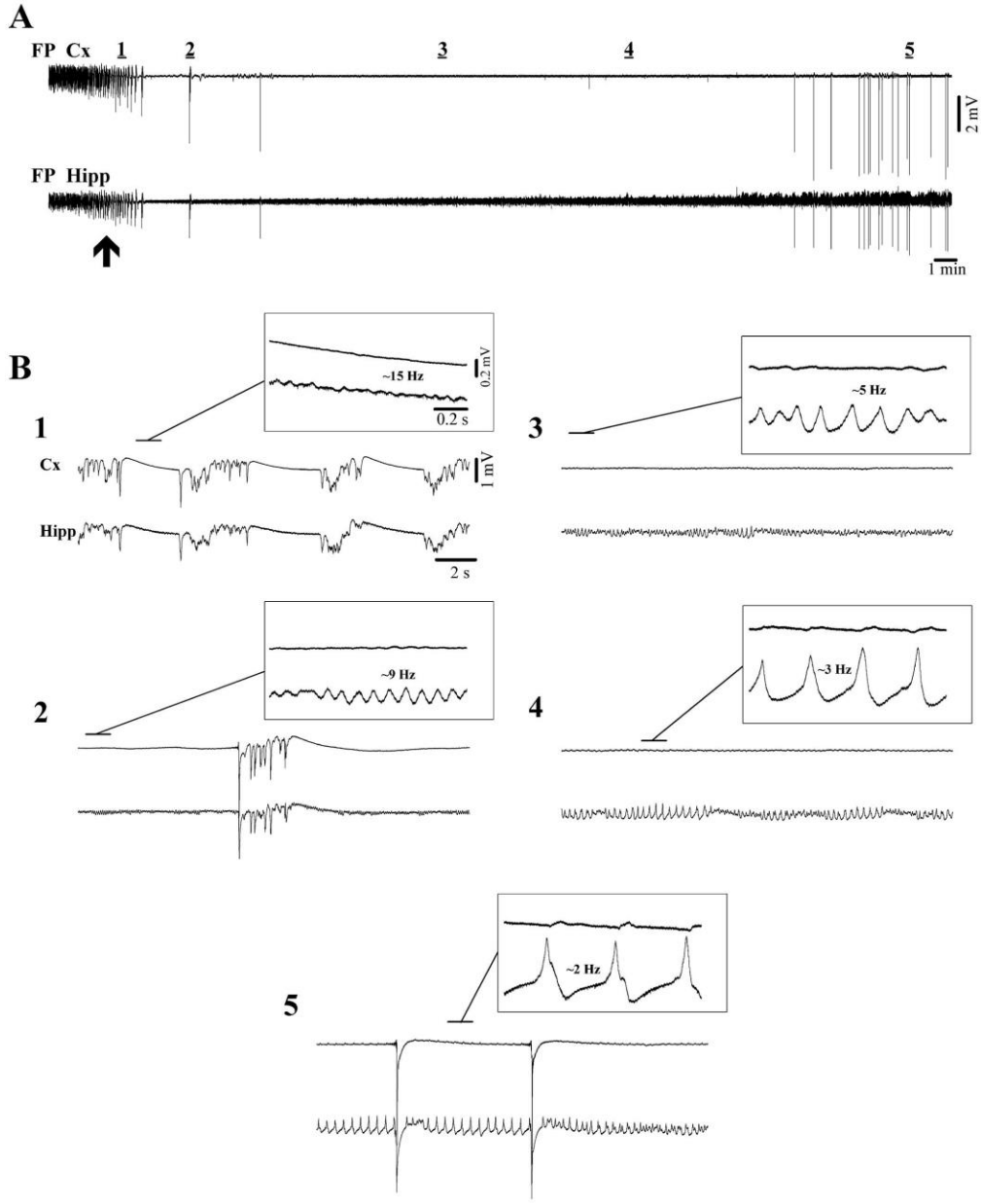

(A) Continuous recordings of intracortical field potentials (FP Cx) together with hippocampal field potentials (FP Hipp) first under lower levels of isoflurane (2%), which is then switched to 4% (at arrow) leading to a gradual suppression of bursting activity and eventually to isoelectric line. The 5 periods underlined by horizontal bars are expanded in (B). (B1) The magnification shows ripple activity in the hippocampus at >15 Hz during transient suppressions. (B2) Isolated burst surrounded by ripple activities in the hippocampus (>9 Hz). (B3) & (B4) Continuous isoelectric line displaying progressively slower and ampler anesthesia ripples in the hippocampal field potential. (B5) C state characterized by ample delta ripples in the hippocampal trace interrupted occasionally by high amplitude νCs. Note that in all insets the overt expression of ripple activities in the cortex is absent. In this figure, all potentials are depicted with positivity upwards.

Cellular correlates of the νC state

Through simultaneous intracellular recordings in the hippocampus and cortex (Figure 8) we could determine that (a) ripple activity was absent in cortical neurons but present in hippocampal cells (Figure 8B), and (b) intracellular νCs spiking occurred first in hippocampal neurons and was then relayed to cortical cells with an average delay of 43 ms (± 4.2) (Figure 8C). Of the 55 neurons recorded, we filled 8 cells with Lucifer Yellow to ascertain the location and morphological features, which allowed subsequent reconstruction with the use of a confocal microscope (Figure 8A). Reconstructed hippocampal cells could be identified as CA3, CA2 and CA1 pyramidal neurons (n = 5), whilst pyramidal shaped and nonpyramidal shaped neurons (aspiny cells) were recovered following cortical recordings (n = 3). All cortical cells displayed steady membrane potentials in-between νCs and did not show any activities related to ripples (Figure 8B). In all recorded cortical neurons (n = 26), EEG νCs were associated with depolarizing membrane potentials crowned by bursts of action potentials (on average 2.6 action potentials/ νC). We suggest that the depolarizing potentials underlying the action potentials are triggered by EPSPs because they increase their amplitude with steady hyperpolarization of the membrane potential (not shown). At the same time, it is unlikely that IPSPs contribute to the shaping of these events since, at lesser isoflurane concentrations than the ones used here cortical inhibition is largely suppressed [42].

Figure 8. Cortical and hippocampal neuronal activity during νC state

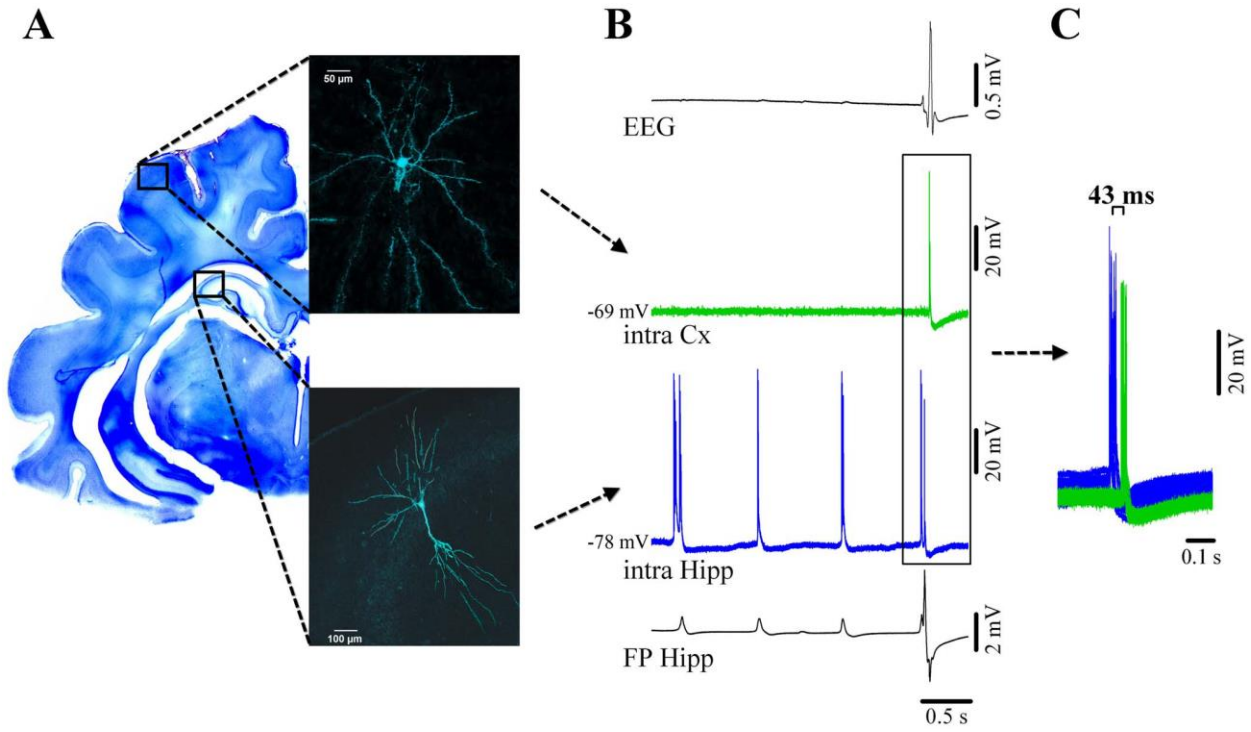

(A) Neocortical pyramidal neuron from suprasylvian area 5 (above) and simultaneously recorded pyramidal CA3 hippocampal neuron filled with Lucifer Yellow and reconstructed with confocal microscopy. Their respective locations are schematically indicated on a Nissl-stained coronal section of the brain. (B) From top to bottom: simultaneous recording of the EEG, intracellular cortical neuron (green), intracellular hippocampal neuron (blue) and adjacent hippocampal field potential (FP). Both hippocampal traces indicate the presence of two types of activities: delta ripples at about 1 Hz (small amplitude positive potentials in the FP, accompanied by bursts of action potentials in the nearby neuron), and a νC (high amplitude spiky multiphasic potential in the FP, which is paralleled by neuronal discharge). The EEG displays a continuous isoelectric line during hippocampal ripples but displays the νC during which the cortical neuron discharges bursts of action potentials. Delta ripples are not expressed in the neocortex. (C) Time relationship between neuronal discharges for νC events indicating that the hippocampal discharges consistently precede the neocortical ones. In this figure, all potentials are depicted with positivity upwards.

Ripple events were exclusively recorded in hippocampal CA3, CA2, and CA1 pyramidal cells (n = 39 pyramidal neurons). Ripples in the delta frequency range with depolarizing bursting activities in hippocampal neurons (on average 3.1 spikes/ripple) were time locked with local field potential events suggesting regional synchrony.

In order to determine whether these events originate from self-sustained oscillations in hippocampal neurons and their intrinsic properties, we applied hyperpolarizing and depolarizing current pulses into the recorded cells. We found that during the νC state hippocampal neurons displayed Ih type currents (Figure 9A left) and bursting capabilities (Figure 9A right). Moreover, when steadily depolarized, hippocampal CA3 neurons spontaneously generated rhythmic bursts. The frequency of these bursts depended foremost on the cell's membrane potential (Figure 9B–C), a finding that meshes well with earlier observations [43]. Thus, changes in the overall network excitatory/inhibitory balance and cellular input levels caused by anesthesia, for example, can modulate the oscillatory frequency of these neurons.

In addition to self-oscillating CA3–1 pyramidal cells, we recorded hippocampal neurons that displayed only minor EPSP responses during delta ripple activity (Figure 10A), despite participating in νC events (n = 6 neurons). According to the stereotaxical coordinates, these neurons were situated in the dentate gyrus (DG). EPSPs related to delta ripples could only be fully revealed by significant hyperpolarization of the membrane potential (Figure 10B), suggesting that delta ripples may have been insufficient in eliciting action potentials in these neurons. We presume these cells to be granule cells from the DG, which exhibit a very high excitability threshold due to the presence of an unusual set of synaptic as well as extrasynaptic non-desensitizing $GABA_A$ receptors [44].

Figure 9. Intrinsic properties of CA3 neurons under isoflurane *in vivo*

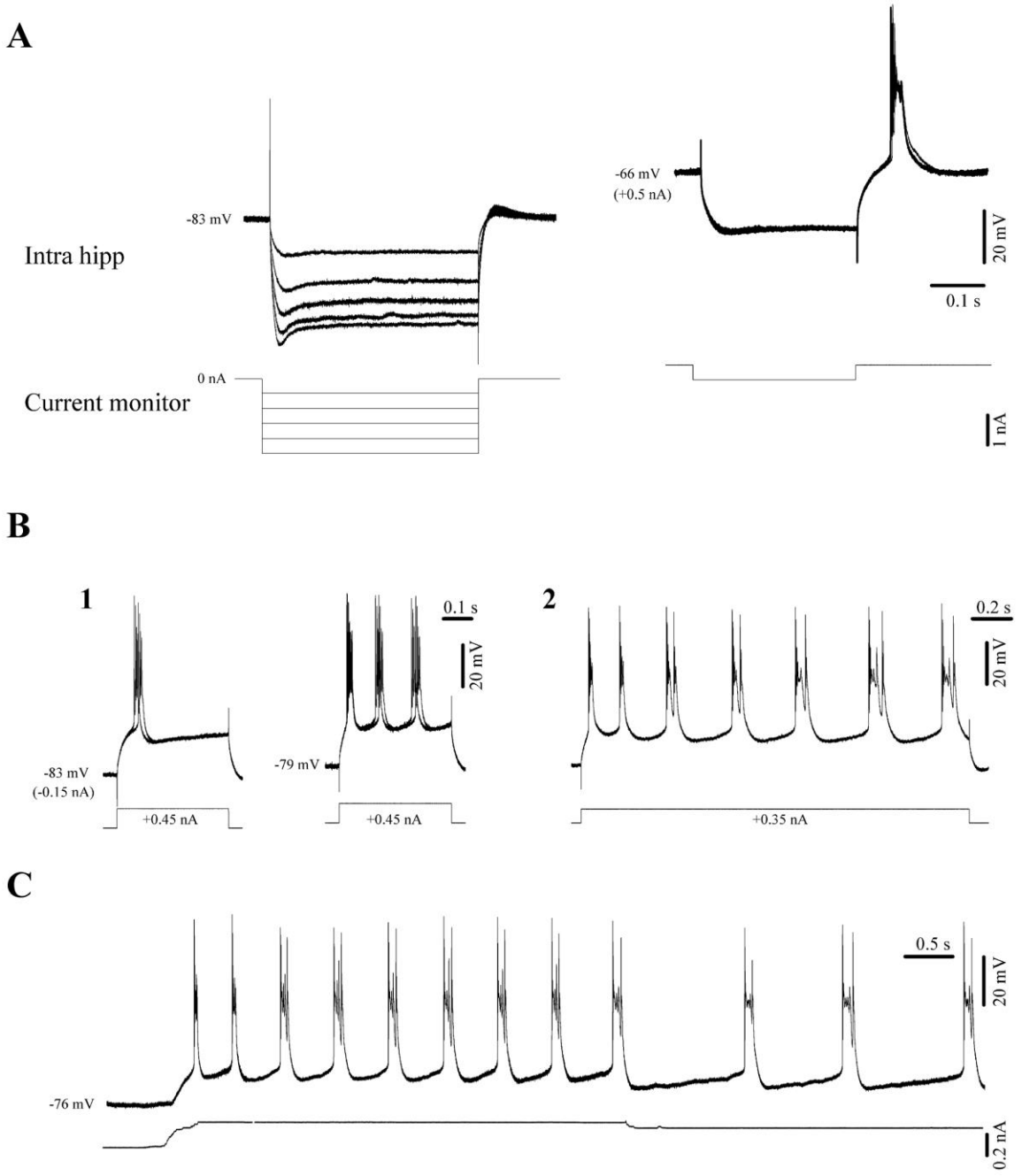

(A) Hyperpolarizing pulses trigger Ih currents which increase with steady hyperpolarization (left). The same cell displayed discharge rebound bursts at more depolarized levels (right). (B) Depolarizing pulses trigger bursts of action potentials (1). Due to their activation characteristics we tentatively regard these bursts as high-threshold spikes (HTS). The HTS responses become rhythmic at more depolarized membrane potentials (1 right). Controlling the cell's membrane polarization modifies the frequency of these oscillations (B2 and C). In this figure, all potentials are depicted with positivity upwards.

Figure 10. Intracellular recording of a putative dentate gyrus granule cell during νC state

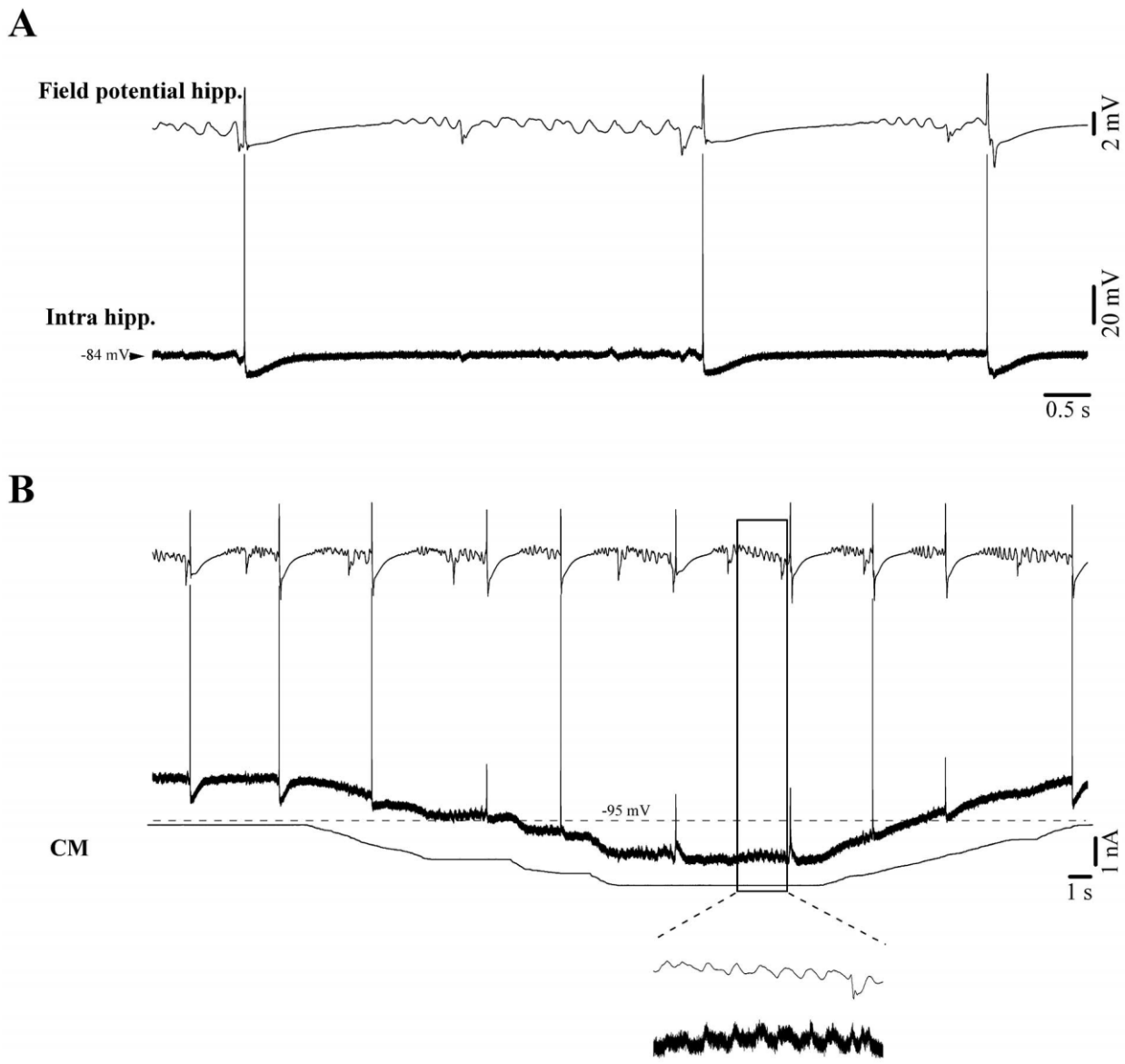

(A) Under resting conditions, the cell discharges bursts of action potentials in relation to νCs. Ripples displayed in the field potential recording (CA3 region) are not overtly paralleled by intracellular potentials. (B) Steady hyperpolarization of the neuronal membrane potential by intracellular current injection to very negative values (beyond -110 mV) reveals phasic events time-locked with the field potential delta ripples. In this figure, all potentials are depicted with positivity upwards.

Synchronization of hippocampal neurons during the NC state

Synchronization is a critical factor for the transmission of hippocampal activity towards the neocortex. Generally, the amplitude of field potentials is considered to reflect the number of

synaptic inputs simultaneously contributing to the coherence of a particular pattern of activity. In the case of delta ripples we assessed the synchronization by measuring the jitter of the onset of neuronal discharge (this onset reflects the point where synaptic inputs from other neurons impose a significant level of depolarization) with respect to the maximum of the positive field potential wave associated with delta ripples (Figure 11A). Depicted in Figure 11A are 10 delta ripples with a dispersion of the first action potential over 44 ms. In the same hippocampal neuron, the equivalent jitter measured for νCs was of only 10 ms (Figure 11B). After performing this comparison in all 39 recorded hippocampal neurons we obtained average jitters of 49.7 ms (±4.8) for delta ripples and 12.4 ms (±1.7) for νCs. The two sets of values were significantly different (signed-rank Wilcoxon test; $p<0.001$).

Figure 11. Synchrony of hippocampal neurons during delta ripples (A) and νCs (B)

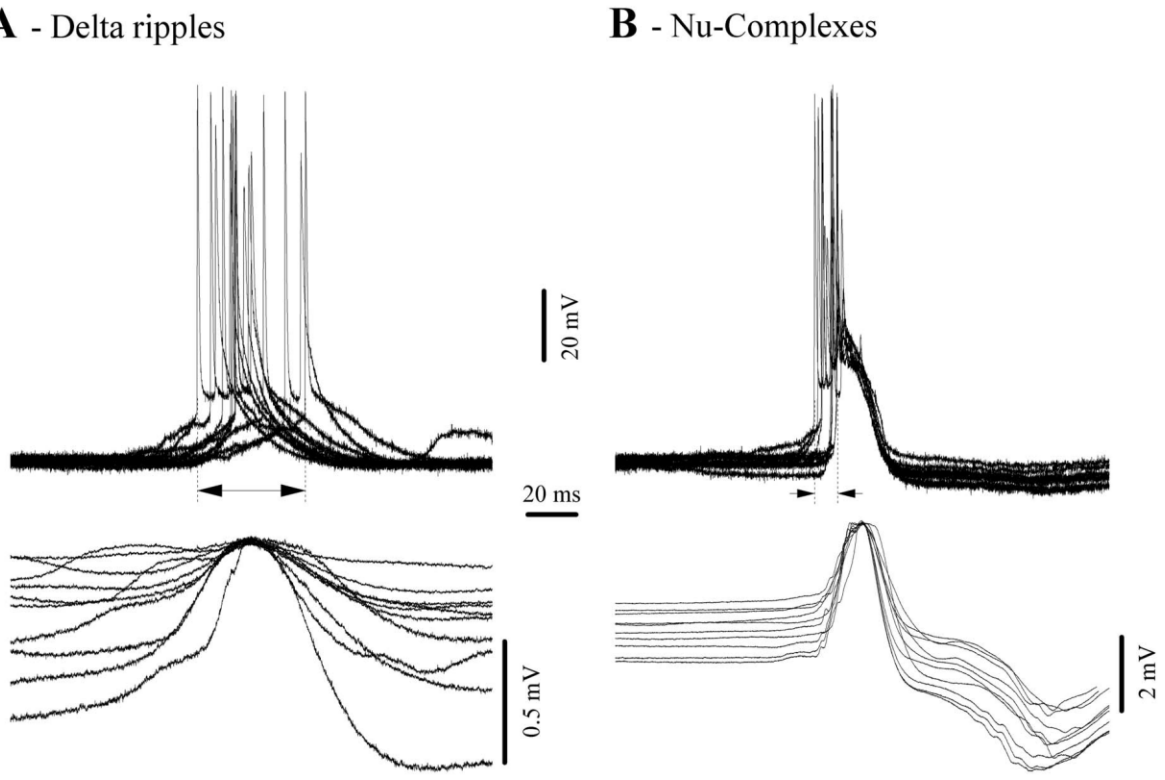

All traces are aligned on the maximum of the field potential. For each panel the vertical dotted lines indicate the earliest and the latest onset of neuronal action potential discharge, whilst the horizontal arrow depicts the dispersion of this onset and represents a measure of the degree of synchrony of hippocampal neurons. In this figure, all potentials are depicted with positivity upwards.

We conclude that the hippocampal networks display greater synchronization during νCs than during delta ripples. This fact may play an important role within the scenario of genesis for νCs and their subsequent hippocampal-neocortical relay of νCs.

Discussion

Study 1

Although subtle seizures have been reported to occur in comatose patients, the semiology of these phenomena, and their relationship to NCSE have not been systematically investigated yet. We have characterized the semiological features of subtle motor phenomena in critically ill patients admitted to the ICU. The most common phenomena were discrete myoclonic twitching and tonic muscle activation.

EEG remained the most robust method to diagnose NCSE. Less than one fourth of patients had NCSE confirmed by EEG, although it was recorded during the subtle convulsions. None of the semiological features could distinguish between the patients with NCSE and those without NCSE. Although it has been suggested that certain features of the subtle movements, like their duration (persistence) can help in distinguishing between NCSE and other causes of these phenomena [6], we could not confirm this in our series. Our results differ from those of a previous study which found that a combination of semiological findings (ocular movement abnormalities), remote risk factors for seizures and severely impaired mental state were seen significantly more often in the patients with NCSE [45]. Therefore, the authors suggested that observation of subtle motor phenomena, in association with clinical data indicating increased risk for seizure can be used to select patients for further diagnostic work-up [45].

A possible explanation for our diverging results might be that discrete motor phenomena, like the ones observed in subtle seizures, have also been reported as side-effects of medications typically used in the ICU, such as anesthetics (propofol, midazolam), antiemetics and corticosteroids [2]. In addition, subtle motor phenomena can occur as a direct consequence of the underlying brain insult in acutely ill patients, such as brainstem and spinal myoclonus, spinal reflexes, automatisms, release signs, posturing movements accompanying cerebral herniation, chorea and hemi-ballismus (due to vascular pathology), asterixis (toxic-metabolic conditions) [46].

A limitation of this study was due to the fact that continuous EEG was not available in the ICUs [47,48]. However, in all cases, EEG was recorded during the subtle motor phenomena documented on the video, and, when necessary, the recordings were repeated. Considering the wide variety of recorded somatotopical features, our sample-size was relatively small. Further larger-scale studies, using continuous EEG recordings are needed to fully elucidate these aspects.

Nevertheless, since less than one fourth of the 60 patients with subtle convulsions had NCSE during these phenomena, it is unlikely that epileptic activity would have caused them.
To the best of our knowledge, this study is the first to systematically address the semiological features of subtle motor phenomena in comatose patients, which can raise the suspicion of NCSE. Nevertheless, EEG is needed to confirm the diagnosis, since none of the semiological features is specific.

Study 2

Using EEG spectral analysis, we confirmed the early observations based on visual evaluation, that reported increase in the slow EEG components at the end of hemodialysis [7,8]. Previous studies using spectral analysis were not able to find such changes [9-12], possibly due to several methodological aspects in these studies. For example, EEG was analyzed for epochs when the patients were performing mental arithmetic exercises, which could have changed the EEG background activity. The power ratio in previous studies was calculated for 3–7 / 7–13 Hz, which does not include a significant portion (0.5–3 Hz) of the delta band. By including the whole delta frequency band, we found a significant increase in its relative power.
Since the 1960s, hemodialysis has proven a lifesaving treatment for patients with CKD. However, a paradoxical change in neurological status was noted in some patients, from the early days of hemodialysis. This deterioration consisted of headache, dizziness, nausea, vomiting, muscular cramps, tremor, convulsions, and altered states of consciousness were described as dialysis disequilibrium syndrome (DDS) [12-15]. These unfavorable changes occurred especially in the first dialysis sessions and appeared when the correction of some biochemical parameters (especially urea) was too rapid. Hence, it was hypothesized that DDS was caused by cerebral edema and increased intracranial pressure, due to difference in osmolality between the rapidly dialyzed serum and the cerebrospinal fluid (CSF) that was lagging behind [7,49].
We found that EEG spectral changes induced by hemodialysis were associated with younger age, recent start of hemodialysis therapy and with the level of uremia, which are similar to the risk factors for DSS mentioned above [12,13]. In addition, we found that lower glycemia before hemodialysis was also associated with an increase in Delta relative power. It is well documented that hypoglycemia causes diffuse EEG slowing and lower glycaemia levels could predispose patients with CKD to the spectral changes during hemodialysis.

When using modern dialysis methods, clinically manifest DDS is a rare phenomenon. Although our patients generally experienced mild symptoms, such as malaise and fatigue at the end of the dialysis sessions, these were not severe and specific enough to be considered as DDS. However, we found significant spectral changes (slowing) after hemodialysis, and these changes were associated with the same risk factors that previously were reported for DSS, suggesting that the spectral changes revealed the pathomechanisms of CNS changes induced by dialysis.

Study 3.

Scenario for the genesis of νCs

From the above data we propose the following scenario to explain how self-oscillations of a limited population of CA3 pyramidal cells can lead to an activity spreading all throughout the brain (Figure 12).

To begin with, hippocampal CA3 neurons have long been known for their tendency to produce highly synchronized population bursts as well as self-sustained rhythmic activity [39,50] due to their intrinsic membrane properties [43] and local inhibitory mechanisms [51]. Under normal conditions, hippocampal CA3 neurons receive finely tuned excitatory and inhibitory inputs from subcortical structures, such as the medial septal nucleus and the diagonal band of Broca [52] generating specific rhythms such as the theta rhythm during exploratory behavior in rats and REM sleep [53]. Thus these neurons are usually under dominant control from afferent inputs, preventing the expression of intrinsically generated firing patterns [54]. The extent of this tightly controlled influence becomes apparent in isolated hippocampal preparations where highly synchronous population bursts are the predominant activity pattern [55].

Figure 12. Schematic for the generation of νCs

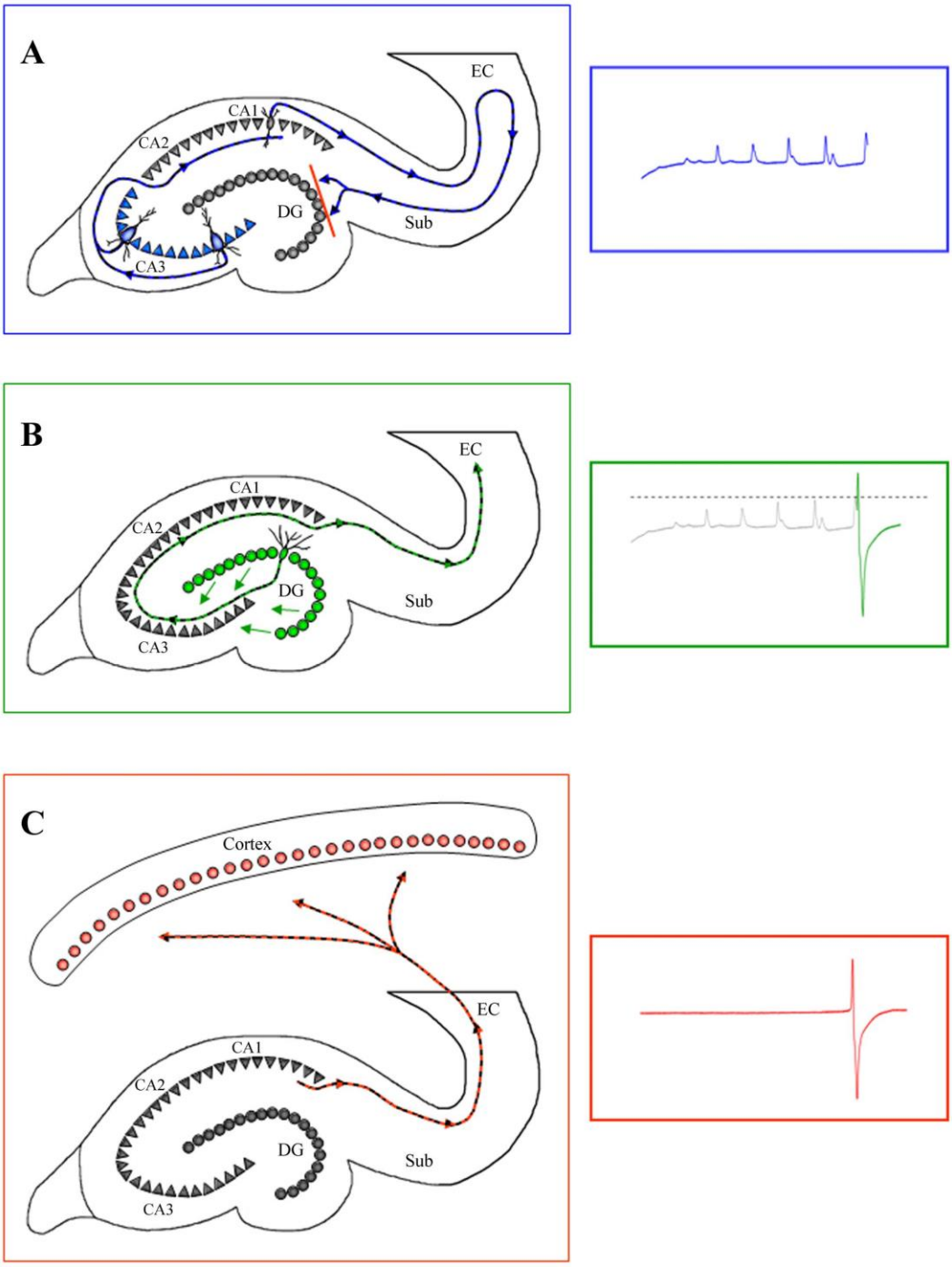

(A) Generation of recurrent delta ripples within hippocampal neurons fails to activate the dentate gyrus. At right: hippocampal field potential activity. (B) Increased synchronization of delta ripples activates dentate gyrus granule cells, which in turn recruit hippocampal neurons, creating a νC. At right, entorhinal cortex field potential activities (green). (C) The newly generated νC activates cortically-projecting deep layers of the entorhinal cortex, permitting the propagation of the νC toward the neocortex. At right, scalp EEG activity.

During anesthesia induced sleep-like patterns and further during BS, control through afferent signaling gradually diminishes, permitting the onset of selfoscillatory activity in CA3 pyramidal neurons [56]. At first, individual cells may follow only their own rhythm; however, through intra-hippocampal connections neighboring cells synchronize their activity and form local ‘‘hot-spots’’ of synchronized activity. Synchronization may also be aided by ephaptic (nonsynaptic) processes i.e. activation of the neighboring cells through changes in the extracellular field when one neuron discharges [57,58], although the only pertinent references stem from studies performed in slices. The increase in synchrony can be observed as an increase in amplitudes of local field potentials of ripple activity during increasing application of isoflurane (Figures 7B1–4 and 12A). Impulses during ripple events travel along the intra-hippocampal loop, similarly to the well studied theta activity during exploratory behaviors. Thus, activity is passed on from the CA3 to CA1 region and from there through the subiculum, to the entorhinal cortex (EC), which presents the main output structure of the hippocampal formation [39].

Deep layers V–VI of the EC project towards cortical targets, whilst superficial layers I–III, send impulses back into the hippocampal loop via the perforant pathway towards the DG [56]. Each of the two populations of EC cells has a specific preferred input frequency: superficial layers I–III respond to activities within the theta range, whilst layers V–VI respond to fast and highly synchronized (140–200 Hz) frequencies such as in sharp waves [59]. Therefore, marginally synchronized ripple events will not be relayed to the cortex by the EC but will be directed towards the hippocampal DG via the perforant pathway. As mentioned above, DG granule cells show very low excitability and have been described as ‘‘gate’’ or ‘‘filter’’ for hippocampal afferent signals [60,61]. Thus the relatively unsynchronized EPSPs of ripples are filtered out by granule cells and their propagation within the hippocampus stops at the DG gate (Fig. 12A). However, since the intra-hippocampal synchrony steadily increases in successive ripple events, the continuous excitation of the granule cell gate by ever increasing volleys leads to a decreasing activation threshold, as granule cells appear to be highly sensitive to preceding signaling activity [62]. Also, CA3 synchronization may have to undergo a certain threshold behavior before singlecell bursting activity leads to a truly synchronous population burst [63]. When this threshold is reached, DG activation is achieved. The divergent connectivity of granule cells [64] ensures their synchronous activation, which in turn results in highly concurrent propagation of the signal towards the rest of the hippocampus via the CA3: a ν-complex is generated (Figure 12B).

This event is then carried through CA2, CA1 and subiculum further towards the EC, where it now activates the deep V–VI layers instead of superficial layers due to the nC's high frequency signal. Consequently, the νC event is further directed towards neocortical targets (Figure 12C) from where it spreads into virtually the whole brain. The propagation of the same event backwards to the hippocampus, or a reverberation of the signal within the hippocampal loop is prevented, as massive population bursts such as νCs result in the activation of strong afterhyperpolarizations in hippocampal principal neurons including granule cells (lasting several hundred milliseconds) shunting the production of further action potentials [51]. This after hyperpolarization is partly due to intrinsic neuronal properties, but is also a result of the inevitable triggering of local inhibitory networks by synchronized population bursts such as sharp waves [39] or νCs. Thus, a phase of silence follows each νC. During this period formerly synchronized CA3 pyramidal neurons lose their collective rhythm and ripple activity is re-set for a new cycle.

Functional implications of the novel n-complex state

In this third part of our study, we described an active brain state that extends well beyond deep coma associated with an EEG isoelectric line and potentially represents a new frontier in brain functioning. We have shown that νCs arise in the hippocampus and are subsequently transmitted to the cortex. The genesis of a hippocampal νC depends upon another hippocampal activity, known as ripple activity, which is not overtly detectable at the cortical level. The νC state is possible due to the intense subcortical activity generated in the hippocampus under conditions where cortical spontaneous functioning is greatly reduced.

These observations have far-reaching consequences:

1) Although in this study the νC state was achieved using the volatile anesthetic isoflurane, the progression from wakefulness to BS and the isoelectric line is similar to other etiologies, anesthesia-induced or not, as is shown by the human data which triggered the subsequent experiments. The two main reasons for employing isoflurane in our study are: (a) the excellent level of control over anesthesia, and (b) its quick reversibility, allowing easy switching between various states. Isoflurane is a lipophilic agent [65], which decreases cerebral metabolism [66] and constitutes one of the most widely employed clinical anesthetics, due to characteristics such as low depression of cardiac contractility, diminished heart rate and arterial pressure, as well as

negligible liver or kidney toxicity [67]. These attributes may have greatly aided our investigation of the νC state in cats, since high concentrations of isoflurane (up to 4%) did neither compromise vital functions (cardiac, respiratory, etc.), nor induce cell death in the brain. Therefore, the νC state represents the deepest form of coma obtained so far, and demonstrates that the brain may remain operational beyond the EEG isoelectric line. However, in many clinical situations, the brain might cease to operate due to anoxic or toxic insults compromising neuronal integrity itself. Our results indicate that if the integrity of neuronal elements is preserved, then the brain may survive. Moreover, the discovery of this novel brain state and its underlying mechanisms draw attention to the difficulties in establishing clinical brain death and could thus revive discussions about the usefulness of depth recordings as an additional assessment criteria for brain death, as suggested by Walker in 1977 [68], to establish the irreversibility of brain damage not only from the scalp level. At the very least, the current findings should serve clinicians in their assessment of patients' depth of coma in case they encounter EEG activity patterns indicative of the νC state. If these patterns were observed, it would be highly advisable to review the patient's medication-regime with regards to coma-deepening drugs. Even though the νC state in our animal studies was fully reversible due to the use of isoflurane anesthesia, other underlying etiologies may be less safe if combined with medication. Therefore, the description and exploration of this phenomenon is potentially life-saving.

2) In our view, the progression toward the νC state emphasizes the following concept related to brain mechanisms: wakefulness, as a state that hosts conscious processes and the domination of willful action is characterized by a predominance of neocortical activity. As these functions fade at the onset of unconsciousness, the orchestrating powers are relinquished to more basic structures such as the thalamus (in the case of sleep) or the limbic system (present data). When these structures are released from neocortical influence, they begin to pursue activity patterns on their own and proceed to impose these patterns on other brain regions including the neocortex. Most of these activity patterns are already present throughout consciousness and unconsciousness. For example, hippocampal oscillations in the theta range in rodents are associated with sensory processing and the control of exploratory behaviors [69]. In our preparation, hippocampal theta oscillations were present during transient isoelectric episodes of BS. The oscillatory frequency then continuously decreased in parallel with the deepening of the coma. This was further paralleled by the slowing of intrinsically generated oscillations as a

function of membrane polarization. Thus, the oscillatory frequency is not simply switched from one particular predetermined frequency band (e.g. theta) to another (e.g. delta) but rather displays a continuous evolution modulated by the depth of coma.

3) The presence of these oscillatory activities in the hippocampus raises some intriguing questions as to their possible involvement in mechanisms of plasticity related to learning and memory processes. The preparation itself and the easy reversibility from νC coma may prove particularly suitable for the testing of the role of hippocampal ripples either in their triggering of sharp waves as a mechanism of reinforcing memory circuits [56], or in downsizing the strength of neuronal connectivity for the purpose of synaptic homeostasis [70].

Conclusions

EEG is an essential tool for diagnosing and characterizing patients with disturbed level of consciousness.

By systematically addressing the semiological features of subtle motor phenomena in comatose patients, we showed that although these phenomena can raise the suspicion of NCSE, EEG is essential to confirm the diagnosis, since none of the semiological features are specific.

We also found that hemodialysis leads to slowing of the EEG background activity and to an increase in the relative power in delta frequency band. This is a potential biomarker for quantifying functional changes in the Central Nervous System during hemodialysis.

Finally, EEG was used to identify a novel rhythm, originating in the hippocampus, in deep coma patients, thereby challenging the common wisdom that the isoelectric line is always associated with absent cerebral activity, and proving that the isoelectric line is not necessarily one of the ultimate signs of a dying brain.

Acknowledgements

I would like to thank Professor Sándor Beniczky for his constant support and high-standard supervision throughout my efforts. I would like to express my gratitude for his guidance to Professor László Vécsei, who so elegantly offers the joy of discovering the fascinating aspects of neurology to his disciples and colleagues. A special place in my academic journey belongs to Professor Florin Amzica from University of Montreal: the very long debates during the very short evenings taught me to raise questions even when everything seemed to be clear. I would like to thank the University of Szeged Doctoral School of Clinical Medicine for making this PhD project possible.

References

1. Treiman D, DeGiorgio C, Salisbury S, Wickboldt C. Subtle generalized convulsive status epilepticus. Epilepsia 1984;25(5):653.

2. Sutter R, Semmlack S, Kaplan PW. Nonconvulsive status epilepticus in adults — insights into the invisible. Nature Reviews Neurology. 2016;12(5):281-93.

3. Treiman DM. Generalized Convulsive Status Epilepticus in the Adult. Epilepsia. 1993;34(s1):S2-S11.

4. Trinka E, Cock H, Hesdorffer D, et al. A definition and classification of status epilepticus – Report of the ILAE Task Force on Classification of Status Epilepticus. Epilepsia. 2015;56(10):1515-23.

5. Rossetti AO, Trinka E, Stähli C, Novy J. New ILAE versus previous clinical status epilepticus semiologic classification: Analysis of a hospital-based cohort. Epilepsia. 2016;57(7):1036-41.

6. Betjemann JP, Lowenstein DH. Status epilepticus in adults. The Lancet Neurology. 2015;14(6):615-24.

7. Kennedy AC, Linton AL, Luke RG, Renfrew S. Electroencephalographic changes during haemodialysis. Lancet. 1963;1(7278):408-11.

8. Hampers CL, Doak PB, Callaghan MN, Tyler HR, Merrill JP. The electroencephalogram and spinal fluid during hemodialysis. Arch Intern Med. 1966;118(4):340-6.

9. Kiley JE, Woodruff MW, Pratt KI. Evaluation of encephalopathy by EEG frequency analysis in chronic dialysis patients. Clin Nephrol. 1976;5(6):245-50.

10. Teschan PE, Ginn HE, Bourne JR, et al. Quantitative indices of clinical uremia. Kidney Int. 1979;15(6):676-97.

11. Basile C, Miller JD, Koles ZJ, Grace M, Ulan RA. The effects of dialysis on brain water and EEG in stable chronic uremia. Am J Kidney Dis. 1987;9(6):462-9.

12. Arieff AI. Dialysis disequilibrium syndrome: current concepts on pathogenesis and prevention. Kidney Int. 1994;45(3):629-35.

13. Patel N, Dalal P, Panesar M. Dialysis disequilibrium syndrome: a narrative review. Semin Dial. 2008;21(5):493-8.

14. Zepeda-Orozco D, Quigley R. Dialysis disequilibrium syndrome. Pediatr Nephrol. 2012;27(12):2205-11.

15. Mistry K. Dialysis disequilibrium syndrome prevention and management. Int J Nephrol Renovasc Dis. 2019;12:69-77.

16. Kroeger D, Amzica F. Hypersensitivity of the anesthesia-induced comatose brain. J Neurosci. 2007;27(39):10597-607.

17. Tétrault S, Chever O, Sik A, Amzica F. Opening of the blood-brain barrier during isoflurane anaesthesia. Eur J Neurosci. 2008;28(7):1330-41.

18. Swank RL, Watson CW. Effects of barbiturates and ether on spontaneous electrical activity of dog brain. J Neurophysiol. 1949;12(2):137-60.

19. Chatrian G. Coma, other states of altered responsiveness, and brain death. In: Daly D, Pedley T, editors. Current Practice in Clinical Electroencephalography. New York: Raven Press; 1990. p. 425-87.

20. Steriade M, Amzica F, Contreras D. Cortical and thalamic cellular correlates of electroencephalographic burst-suppression. Electroencephalogr Clin Neurophysiol. 1994;90(1):1-16.

21. Brenner RP. The interpretation of the EEG in stupor and coma. Neurologist. 2005;11(5):271-84.

22. Davis H. Electrical activity of the brain: its relationship to physiological states and states of impaired consciousness. Res Publ Assoc Nerv Ment. 1939;19:50-80.

23. Fischgold H, Mathis P, clinique Fidéedn. Obnubilations, comas et stupeurs: études électroencéphalographiques par H. Fischgold ... et P. Mathis: Masson et Cie (Niort, impr. Soulisse et Cassegrain); 1959.

24. Teasdale G, Jennett B. Assessment of coma and impaired consciousness. A practical scale. Lancet. 1974;2(7872):81-4.

25. ***. Guidelines for the determination of death. Report of the medical consultants on the diagnosis of death to the President's Commission for the Study of Ethical Problems in Medicine and Biomedical and Behavioral Research. Jama. 1981;246(19):2184-6.

26. Beniczky S, Hirsch LJ, Kaplan PW, et al. Unified EEG terminology and criteria for nonconvulsive status epilepticus. Epilepsia. 2013;54(s6):28-9.

27. Leitinger M, Trinka E, Gardella E, et al. Diagnostic accuracy of the Salzburg EEG criteria for non-convulsive status epilepticus: a retrospective study. The Lancet Neurology. 2016;15(10):1054-62.

28. Leitinger M, Beniczky S, Rohracher A, et al. Salzburg Consensus Criteria for Non-Convulsive Status Epilepticus – approach to clinical application. Epilepsy & Behavior. 2015;49:158-63.

29. Jasper HH. The 10-20 electrode system of the International Federation. Electroenceph Clin Neurophysiol. 1958;10:370-5.

30. Kim J. Bimodal emotion recognition using speech and physiological changes. In: Grimm M, Kroschel K, editors. Robust Speech Recognition and Understanding. Vienna, Austria: I-Tech Education and Publishing; 2007. p. 265-80.

31. Steriade M. Grouping of brain rhythms in corticothalamic systems. Neuroscience. 2006;137(4):1087-106.

32. Steriade M, Nuñez A, Amzica F. A novel slow (< 1 Hz) oscillation of neocortical neurons in vivo: depolarizing and hyperpolarizing components. J Neurosci. 1993;13(8):3252-65.

33. Brenner RP. The electroencephalogram in altered states of consciousness. Neurol Clin. 1985;3(3):615-31.

34. Niedermeyer E. The burst-suppression electroencephalogram. Am J Electroneurodiagnostic Technol. 2009;49(4):333-41.

35. Pagni CA, Courjon J. Electroencephalographic modifications induced by moderate and deep hypothermia in man Acta Neurochir Suppl. 1964;14:Suppl 13:35-49.

36. Silverman D. The electroencephalogram in anoxic coma. In: Rémond A, Editor. Handbook of electroencephalography and clinical neurophysiology. Amsterdam: Elsevier; 1975. p. 81-94.

37. Weissenborn K, Wilkens H, Hausmann E, Degen PH. Burst suppression EEG with baclofen overdose. Clin Neurol Neurosurg. 1991;93(1):77-80.

38. Zaret BS. Prognostic and neurophysiological implications of concurrent burst suppression and alpha patterns in the EEG of post-anoxic coma. Electroencephalogr Clin Neurophysiol. 1985;61(4):199-209.

39. Buzsáki G. Hippocampal sharp waves: their origin and significance. Brain Res. 1986;398(2):242-52.

40. Nuñez A, García-Austt E, Buño W. Slow intrinsic spikes recorded in vivo in rat CA1–CA3 hippocampal pyramidal neurons. Experimental Neurology. 1990;109(3):294-9.

41. Ayala GF, Dichter M, Gumnit RJ, Matsumoto H, Spencer WA. Genesis of epileptic interictal spikes. New knowledge of cortical feedback systems suggests a neurophysiological explanation of brief paroxysms. Brain Res. 1973;52:1-17.

42. Ferron JF, Kroeger D, Chever O, Amzica F. Cortical inhibition during burst suppression induced with isoflurane anesthesia. J Neurosci. 2009;29(31):9850-60.

43. Hablitz JJ, Johnston D. Endogenous nature of spontaneous bursting in hippocampal pyramidal neurons. Cellular and Molecular Neurobiology. 1981;1(4):325-34.

44. Coulter DA, Carlson GC. Functional regulation of the dentate gyrus by GABA-mediated inhibition. Prog Brain Res. 2007;163:235-43.

45. Husain AM, Horn GJ, Jacobson MP. Non-convulsive status epilepticus: usefulness of clinical features in selecting patients for urgent EEG. J Neurol Neurosurg Psychiatry. 2003;74(2):189-91.

46. Hannawi Y, Abers M, Geocadin R, Mirski M. Abnormal movements in critical care patients with brain injury: A diagnostic approach. Critical Care. 2016;20.

47. Claassen J, Taccone FS, Horn P, Holtkamp M, Stocchetti N, Oddo M. Recommendations on the use of EEG monitoring in critically ill patients: consensus statement from the neurointensive care section of the ESICM. Intensive Care Medicine. 2013;39(8):1337-51.

48. Herman ST, Abend NS, Bleck TP, et al. Consensus statement on continuous EEG in critically ill adults and children, part I: indications. J Clin Neurophysiol. 2015;32(2):87-95.

49. Port FK, Johnson WJ, Klass DW. Prevention of dialysis disequilibrium syndrome by use of high sodium concentration in the dialysate. Kidney Int. 1973;3(5):327-33.

50. Kandel ER, Spencer WA. Electrophysiology of hippocampal neurons. II. After-potentials and repetitive firing. J Neurophysiol. 1961;24:243-59.

51. Biscoe TJ, Duchen MR. An intracellular study of dentate, CA1 and CA3 neurones in the mouse hippocampal slice. Q J Exp Physiol. 1985;70(2):189-202.

52. Fernández de Sevilla D, Buño W. Presynaptic inhibition of Schaffer collateral synapses by stimulation of hippocampal cholinergic afferent fibres. Eur J Neurosci. 2003;17(3):555-8.

53. Zhang H, Lin SC, Nicolelis MA. Spatiotemporal coupling between hippocampal acetylcholine release and theta oscillations in vivo. J Neurosci. 2010;30(40):13431-40.

54. Buzsáki G, Lai-Wo S L, Vanderwolf CH. Cellular bases of hippocampal EEG in the behaving rat. Brain Research Reviews. 1983;6(2):139-71.

55. Buzsáki G, Gage FH, Kellényi L, Björklund A. Behavioral dependence of the electrical activity of intracerebrally transplanted fetal hippocampus. Brain Res. 1987;400(2):321-33.
56. Buzsáki G. Two-stage model of memory trace formation: a role for "noisy" brain states. Neuroscience. 1989;31(3):551-70.
57. Dudek FE, Snow RW, Taylor CP. Role of electrical interactions in synchronization of epileptiform bursts. Adv Neurol. 1986;44:593-617.
58. Taylor CP, Dudek FE. Synchronous neural afterdischarges in rat hippocampal slices without active chemical synapses. Science. 1982;218(4574):810-2.
59. Chrobak JJ, Buzsáki G. Selective activation of deep layer (V-VI) retrohippocampal cortical neurons during hippocampal sharp waves in the behaving rat. J Neurosci. 1994;14(10):6160-70.
60. Andersen P, Holmqvist B, Voorhoeve PE. Entorhinal activation of dentate granule cells. Acta Physiol Scand. 1966;66(4):448-60.
61. Dudek FE, Sutula TP. Epileptogenesis in the dentate gyrus: a critical perspective. Prog Brain Res. 2007;163:755-73.
62. Heinemann U, Beck H, Dreier JP, Ficker E, Stabel J, Zhang CL. The dentate gyrus as a regulated gate for the propagation of epileptiform activity. Epilepsy Res Suppl. 1992;7:273-80.
63. de la Prida LM, Huberfeld G, Cohen I, Miles R. Threshold behavior in the initiation of hippocampal population bursts. Neuron. 2006;49(1):131-42.
64. Claiborne BJ, Amaral DG, Cowan WM. A light and electron microscopic analysis of the mossy fibers of the rat dentate gyrus. J Comp Neurol. 1986;246(4):435-58.
65. Lerman J, Schmitt-Bantel BI, Gregory GA, Willis MM, Eger EI, 2nd. Effect of age on the solubility of volatile anesthetics in human tissues. Anesthesiology. 1986;65(3):307-11.
66. Newberg LA, Milde JH, Michenfelder JD. The cerebral metabolic effects of isoflurane at and above concentrations that suppress cortical electrical activity. Anesthesiology. 1983;59(1):23-8.
67. Eger EI, 2nd. The pharmacology of isoflurane. Br J Anaesth. 1984;56 Suppl 1:71s-99s.
68. Walker AE. Cerebral Death. Dallas: Professional Information Library; 1977.
69. Buzsáki G. The hippocampo-neocortical dialogue. Cereb Cortex. 1996;6(2):81-92.
70. Tononi G, Cirelli C. Sleep function and synaptic homeostasis. Sleep Med Rev. 2006;10(1):49-62.